Alignment-Dependent Fluorescence Emission Induced by Tunnel Ionization of Carbon Dioxide from Lower-Lying Orbitals

Jinping Yao,[1] Guihua Li,[1,7] Xinyan Jia,[2] Xiaolei Hao,[3,4] Bin Zeng,[1] Chenrui Jing,[1,7] Wei Chu,[1] Jielei Ni,[1,7] Haisu Zhang,[1,7]
Hongqiang Xie,[1,7] Chaojin Zhang,[1] Zengxiu Zhao,[5] Jing Chen,[3,4,*] Xiaojun Liu,[6,†] Ya Cheng,[1,‡] and Zhizhan Xu[1,§]

[1]*State Key Laboratory of High Field Laser Physics, Shanghai Institute of Optics and Fine Mechanics,*
Chinese Academy of Sciences, Shanghai 201800, China
[2]*Quantum Optoelectronics Laboratory, Southwest Jiaotong University, Chengdu 610031, China*
[3]*Key Laboratory of High Energy Density Physics Simulation, Center for Applied Physics and Technology,*
Peking University, Beijing 100084, China
[4]*Institute of Applied Physics and Computational Mathematics, Beijing 100088, China*
[5]*Department of Physics, National University of Defense Technology, Changsha 410073, China*
[6]*State Key Laboratory of Magnetic Resonance and Atomic and Molecular Physics, Wuhan Institute of Physics*
and Mathematics, Chinese Academy of Sciences, Wuhan 430071, China
[7]*University of Chinese Academy of Sciences, Beijing 100049, China*

The study of the ionization process of molecules in an intense infrared laser field is of paramount interest in strong-field physics and constitutes the foundation of imaging of molecular valence orbitals and attosecond science. We show measurement of alignment-dependent ionization probabilities of the lower-lying orbitals of the molecules by experimentally detecting the alignment dependence of fluorescence emission from tunnel ionized carbon dioxide molecules. The experimental measurements are compared with the theoretical calculations of the strong field approximation and molecular Ammosov-Delone-Krainov models. Our results demonstrate the feasibility of an all-optical approach for probing the ionization dynamics of lower-lying orbitals of molecules, which is until now still difficult to achieve by other techniques. Moreover, the deviation between the experimental and theoretical results indicates the incompleteness of current theoretical models for describing strong field ionization of molecules.

Tunnel ionization is a fundamental mechanism underlying the extreme nonlinear strong field atomic and molecular phenomena such as high-order harmonic generation (HHG), above-threshold ionization (ATI), etc. [1–6]. The sensitivities of tunnel ionization on the ionization potential as well as the orbital structures and symmetries render itself an efficient probe of the electronic structures of molecules in either a static or a dynamic manner [7,8]. Based on this expectation, considerable effort has been devoted to unlocking the geometric information of the highest occupied molecular orbitals (HOMOs) of molecules from their alignment-dependent tunnel ionization rates [9–11]. Indeed, for some molecules such as N_2 and O_2, satisfying agreement between the experimental and theoretical results has been obtained. However, when examining the carbon dioxide (CO_2) molecules, the alignment-dependent ionization rate of its HOMO orbital calculated using the molecular Ammosov-Delone-Krainov (MO-ADK) theory fails to reproduce the experimental observation [9]. Moreover, a recent study of the wavelength dependence of tunnel ionization of O_2 in strong laser fields confirms that interference between the electron wave packets ionized from different cores, which is not included in the MO-ADK theory, actually plays an important role [12]. These facts indicate the complexity of

ionization mechanisms of molecules in strong laser fields. Although experimental investigations of tunnel ionization of molecules are frequently carried out based on high-order harmonic generation or above-threshold ionization techniques, they usually lack the capability to directly access the lower-lying orbitals of molecules due to the difficulties in distinguishing the contributions to the total ionization rate from the individual orbitals. On the other hand, for some molecules, their lower-lying orbitals can substantially contribute to the ionization process [13–17]. Therefore, establishment of a technique that allows direct observation of tunnel ionization from individual lower-lying orbitals will undoubtedly be of great importance. In this Letter, we show that such an ambition can be realized by employing the fact that the intensities of the fluorescence lines directly reflect the ionization probabilities from lower-lying molecular orbitals [18,19]. By measuring the alignment dependence of fluorescence, one can obtain the alignment dependence of ionization probability from HOMO-1 and HOMO-2 orbitals.

In our alignment-dependent fluorescence experiment, CO_2 was chosen mainly because its ionization mechanism in the tunnel regime has been a long-standing controversial issue and a topic of hot debate, making it an attractive candidate [9,20]. The pump and probe pulses were

obtained by splitting linearly polarized output laser pulses (800 nm, ~40 fs, 1 kHz, 6 mJ) from a Ti:sapphire laser system (Legend Elite-Duo, Coherent Inc.) using a 50% beam splitter. The pump beam, which was used for aligning the molecules, passed through an inverted telescope for reducing its beam diameter by half. Then, the two beams were recombined by a 50% beam splitter and collinearly focused by a lens into a chamber filled with CO_2 gas. In order to gain a high degree of alignment at the room temperature, the pump beam was slightly broadened to ~60 fs, whereas the pulse duration of the probe beam was maintained at ~40 fs. Because of its smaller beam size, the peak intensity of the pump beam at the focal spot is significantly lower than that of the probe beam, as we attempt to minimize the fluorescence signal (i.e., the ionization) produced by the pump pulse alone. Meanwhile, special care was taken to choose a relatively low gas pressure of ~2 mbar to minimize both the influence of plasma defocusing but also the contribution from collisional excitation [21,22]. Under such a low gas pressure condition, the plasma defocusing effect can be safely ignored as we have confirmed in our experiment. A delay line and a half-wave plate were inserted into the pump-beam path for adjusting the time delay and the relative angle between the polarization axes of the pump and probe pulses, respectively. The fluorescence spectra of CO_2^+ were collected from the backward direction (i.e., opposite to the direction of laser propagation) using a fused silica lens and then were detected by a grating spectrometer (Shamrock 303i, Andor). With this scheme, the alignment dependence of spontaneous emission, which leads to anisotropic fluorescence emission around the optical axis of the laser beam, could be minimized, and thus the measurement of the fluorescence signal as a function of the molecular alignment angle is equivalent to measurement of the alignment-dependent ionization probability of molecules from their corresponding lower-lying orbitals. In our experiment, the peak intensity of the probe pulses at the focus was set at ~4×10^{14} W/cm², resulting in a Keldysh parameter $\gamma \approx 0.6$ calculated using the ionization potential of HOMO-1 of CO_2. This ensures that the ionization processes investigated here all occur in the tunnel regime.

From the electronic configuration of neutral CO_2 molecules $(1\sigma_g)^2(1\sigma_u)^2(2\sigma_g)^2(3\sigma_g)^2(2\sigma_u)^2(4\sigma_g)^2(3\sigma_u)^2 \times (1\pi_u)^4(1\pi_g)^4$, we find that removal of electrons from HOMO-1 (i.e., the $1\pi_u$ orbital) and HOMO-2 (i.e., the $3\sigma_u$ orbital) of CO_2 will produce CO_2^+ in the first $(A^2\Pi_u)$ and the second excited states $(B^2\Sigma_u)$, respectively. Decay from these excited states to the ground state $(X^2\Pi_g)$ will lead to spontaneous fluorescence emissions at 338 nm $(A^2\Pi_u \rightarrow X^2\Pi_g, 1 \rightarrow 0)$ and 289 nm $(B^2\Sigma_u \rightarrow X^2\Pi_g, 0 \rightarrow 0)$, as illustrated in Fig. 1(a). A typical fluorescence spectrum from the unaligned CO_2 molecules measured by the grating spectrometer is shown in Fig. 1(b). Throughout
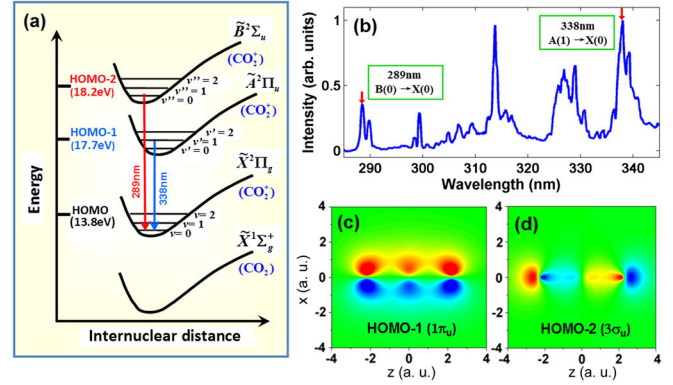

FIG. 1 (color online). (a) Energy level diagram of ionized and neutral CO_2 molecules. The fluorescence emissions at wavelengths of 338 and 289 nm originate from the transitions $(A^2\Pi_u \rightarrow X^2\Pi_g, 1 \rightarrow 0)$ and $(B^2\Sigma_u \rightarrow X^2\Pi_g, 0 \rightarrow 0)$. (b) A typical fluorescence spectrum measured using a grating spectrometer. Calculated electron wave packets of lower-lying orbitals of CO_2 by the GAMESS code shown in (c) HOMO-1, and (d) HOMO-2.

the experiment, a 1200 grooves/mm grating and a 300 μm slit were used, and thus the spectral resolution in the range of 280–350 nm was ~0.07 nm. We chose two fluorescence lines at wavelengths of 338 and 289 nm for investigating the ionizations of CO_2 from the HOMO-1 and HOMO-2, respectively. The wave functions of HOMO-1 and HOMO-2 of CO_2 molecules were calculated using the GAMESS code [23] as illustrated in Figs. 1(c) and 1(d), respectively.

Figures 2(a) and 2(b) show the measured fluorescence signals at the respective wavelengths of 338 and 289 nm as functions of the time delay between the pump and probe pulses. To augment the details in the variation of the fluorescence signal with the changing time delay, the time range in Fig. 2 is confined to half of the rotational period T_{rot} ($T_{rot} \approx 42.7$ ps). Here, the zero time delay ($t = 0$), which corresponds to the best temporal overlap between the pump and probe pulses, was determined by maximizing the white light generation in air. To achieve a high degree of alignment and keep the background fluorescence signal as weak as possible, the diameter and the intensity of the pump beam were carefully optimized. The polarization directions of the pump and probe pulses were set to be parallel to each other. Figure 2(c) shows the calculated temporal evolution of the degree of alignment $\langle\cos^2\theta\rangle$ of CO_2 molecules, which is defined as $\langle\cos^2\theta\rangle \equiv \sum_{J_0=0}^{\infty} g_{J_0} \sum_{M_0=-J_0}^{J_0} \langle\cos^2\theta\rangle_{J_0,M_0}$, by assuming an initial Boltzmann distribution of the molecular ensemble. Here, θ is the angle between the molecular axis and the polarization direction of pump pulses. Under this condition, we have $\langle\cos^2\theta\rangle_{J_0,M_0} = \langle\Psi(t)|\cos^2\theta|\Psi(t)\rangle$, and g_{J_0} is the Boltzmann weights of the initial state $|J_0, M_0\rangle$. For the nonadiabatic field-free alignment, the rotational wave
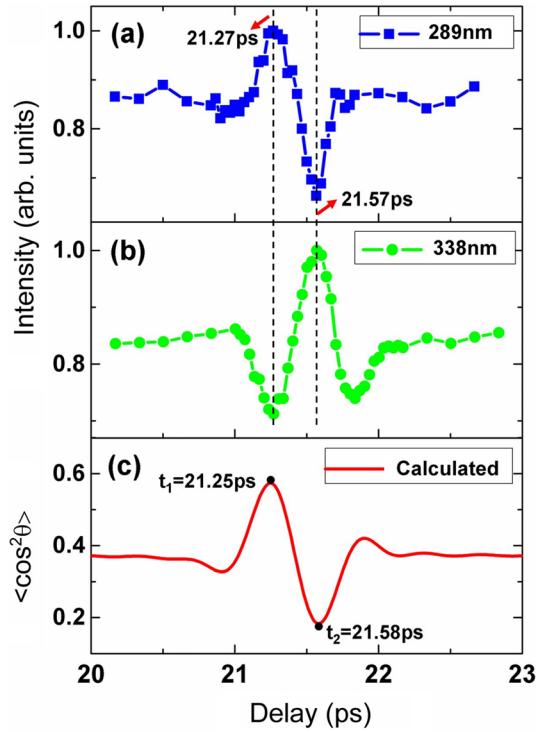
FIG. 2 (color online).   Temporal evolution of the fluorescence signals at (a) 289 and (b) 338 nm wavelengths from aligned CO_2 molecules at the moment around the first half-revival. (c) The calculated time-dependent alignment parameter $\langle\cos^2\theta\rangle$.

packet $\Psi(t)$ is calculated by solving the time-dependent Schrödinger equation based on the rigid rotor model [24,25]. In our simulation, the parameters were the same as the experimental ones (i.e., 800 nm, 60 fs, 1×10^{14} W/cm^2, 300 K). In Fig. 2(c), it can be seen that at $t_1 = 21.25$ ps, the molecule ensemble is aligned in the direction parallel to the polarization of pump pulses, whereas at $t_2 = 21.58$ ps, an antialigned ensemble is generated, namely, the molecular axis is perpendicular to the polarization of pump pulses. Apparently, the experimental observations shown in Figs. 2(a) and 2(b), i.e., the changes of the fluorescence intensities with the time delay, show a strong similarity with the theoretical curve in Fig. 2(c). The evolution of the fluorescence signal at 289 nm follows the same trend of the theoretical curve, whereas the evolution of the fluorescence signal at 338 nm shows an opposite dependence on the time-dependent alignment degree. This finding reflects the difference in the alignment dependence of ionization rates of CO_2 from the HOMO-1 and HOMO-2. The fluorescence at 338 nm originates from HOMO-1 with a π_u symmetry which has a nodal plane along the direction parallel to the molecular axis, and thus this signal becomes the weakest when the parallel alignment was achieved due to the suppressed ionization [26]. In contrast, the 289 nm signal originates from HOMO-2 with a σ_u symmetry; thus, it reached its maximum under the parallel alignment condition. The fluorescence signal at

289 nm wavelength reaches its maximum and minimum at the time delay of 21.27 and 21.57 ps, respectively. In contrast, the situation for the fluorescence signal at 338 nm is completely opposite.

By measuring the fluorescence signal as a function of the alignment angle, the alignment dependence of the ionization probability from an individual lower-lying orbital can be directly examined. As indicated by the black dashed line in Fig. 2, the parallel alignment of the ensemble of CO_2 molecules was achieved at the time delay of 21.27 ps. The alignment dependence of fluorescence intensity can thus be examined by varying the relative angle α between the pump polarization and the probe polarization at this fixed time delay, which was achieved by rotating the pump polarization direction with a half-wave plate for the probe polarization being fixed in the horizontal direction. Figures 3(a) and 3(b) present the measured fluorescence intensities at the wavelengths of 338 and 289 nm, respectively, as a function of the angle α. In Figs. 3(a) and 3(b), a weak fluorescence background generated by the pump pulses alone has been subtracted from the total fluorescence signal. Monotonic increase of the fluorescence signal at 338 nm is observed for an angular range from 0° to 90°, whereas the signal at 289 nm exhibits a different behavior; i.e., it decreases with the increasing angle α. This behavior can be attributed to the sensitivity of tunnel ionization on the geometries of molecular orbitals.

The measured alignment-dependent fluorescence intensity $S_{\exp}(\alpha, t = 21.27 \text{ ps})$ in Fig. 3 can be regarded as the convolution of the alignment-dependent ionization probability $P_{\text{ion}}(\theta')$ and the time-dependent distribution of aligned molecular axis $\rho(\theta, t_1)$ [7,9]; thus, it can be expressed as

$$S_{\text{cal}}(\alpha, t_1) = \int_{\varphi'=0}^{2\pi} \int_{\theta'=0}^{\pi} \rho(\theta(\theta', \varphi', \alpha), t_1) P_{\text{ion}}(\theta')$$
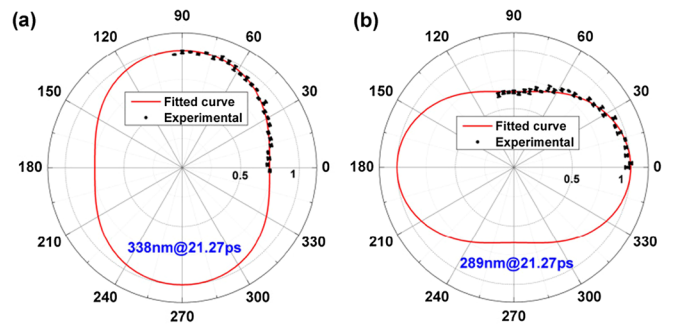$$\times \sin\theta' d\theta' d\varphi'. \tag{1}$$

FIG. 3 (color online).   Fluorescence signals at (a) 338 and (b) 289 nm as functions of the relative polarization angle α between pump and probe pulses at the time delay of 21.27 ps. The error bars in the fluorescence signals are estimated from multiple measurements. Red solid lines are corresponding theoretical fitting curves.

Here, $\rho(\theta, t_1) = \sum_{J_0=0}^{\infty} g_{J_0} \sum_{M_0=-J_0}^{J_0} \langle \Psi(t)|\Psi(t)\rangle|_{t=t_1}$ is calculated by solving the time-dependent Schrödinger equation at the moment of the first half-revival ($t_1 = 21.25$ ps) with the same parameters as used in Fig. 2(c). The time-dependent distribution $\rho(\theta, t_1)$ in the frame of pump pulses can be transformed to the frame of probe pulses using the relation $\cos\theta = \cos\alpha \cos\theta' + \sin\alpha \sin\theta' \cos\varphi'$, where θ' and φ' are the polar and azimuthal angles in the frame of probe pulses, respectively. To retrieve the alignment-dependent ionization probability $P_{ion}(\theta')$, we first expand it into the form $P_{ion}(\theta') = \sum_{n=0}^{3} C_n \cos(2n\theta')$, and then determine the coefficients C_n by fitting the calculated $S_{cal}(\alpha, t_1)$ to the measured $S_{exp}(\alpha, t = 21.27 \text{ ps})$. As indicated by the red solid lines in Figs. 3(a) and 3(b), the calculated fluorescence signal $S_{cal}(\alpha, t_1)$ are in good agreement with the measured curves.

Generally, besides *ab initio* methods [10], two analytical models, i.e., the strong-field-approximation (SFA) theory [27–29] and MO-ADK theory [3], have been widely applied to describe the molecular ionization in strong laser fields. However, the underlying physical pictures of the ionization process are intrinsically different in these two models. The MO-ADK theory treats the ionization of molecules as a tunneling process which is essentially identical to that of atoms. Hence, the ionization is mainly determined by the asymptotic behavior of the bound state wave function at large distance [3]. However, in the SFA theory, the ionization is calculated by the S-matrix theory which treats the external laser field in a nonperturbative way. For molecules like O_2, the interference between ionized wave packets emitted from different nuclei in the molecule is believed to play an essential role in the ionization process [12,27]. On the other hand, study of the alignment-dependent total ionization probability of CO_2 with ion measurement shows significant deviation from the prediction of the MO-ADK theory [9] and leads to intensive investigations [10,30,31].

To shed more light on this controversial problem and check the validity of our experiment method, we compare the retrieved alignment-dependent ionization probabilities from both the HOMO-1 and HOMO-2 with simulation results of the length-gauge SFA theory and MO-ADK theory in Fig. 4. In these calculations, ionization rates of electrons from the HOMO-1 and HOMO-2 are evaluated using the formulas in Refs. [28,29] (for length-gauge SFA) and Ref. [3] (for MO-ADK). The wave functions are obtained by GAMESS code [Figs. 1(c) and 1(d)]. For the HOMO-1 in Fig. 4(a), the deconvoluted $P_{ion}(\theta')$, which gives rise to the fluorescence signal at 338 nm, shows a heart-shaped distribution with the ionization probability peaked at $\sim 65°$, which is consistent with the prediction of the SFA calculation. It is intriguing that similar to the alignment-dependent total ionization probability of CO_2 shown in Ref. [9], our results significantly differ from that given by the MO-ADK theory. Note that the laser
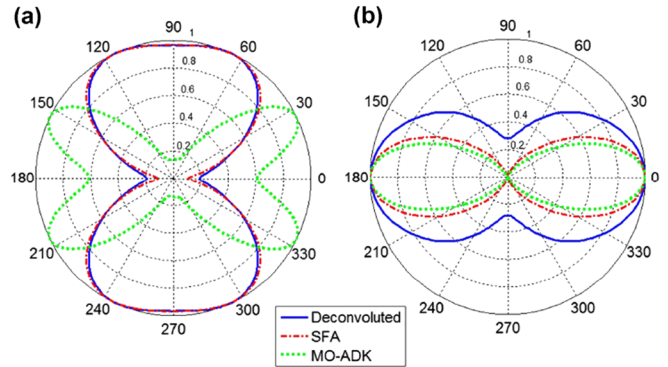

FIG. 4 (color online). Experimentally retrieved alignment-dependent ionization probability $P_{ion}(\theta')$ of CO_2 molecules (blue solid lines) for (a) HOMO-1 and (b) HOMO-2. Corresponding results obtained using the length-gauge SFA and the MO-ADK calculations are indicated by the red dot-dashed lines and the green dotted lines, respectively.

parameters used in our experiment ensure that the ionization happens in the tunneling regime ($\gamma \approx 0.6$ for HOMO-1), different from that used in Ref. [9] which is about $\gamma \approx 1$ and the multiphoton effect may affect the ionization process. The MO-ADK calculation for HOMO-1 shows that the alignment-dependent ionization probability peaks at $\sim 30°$ as shown in Fig. 4(a), which coincides with the peak of the angular distribution of the asymptotic electron density of CO_2. For the HOMO-2 in Fig. 4(b), the deconvoluted $P_{ion}(\theta')$ (retrieved at 289 nm), gradually decreases from 0° to 90°, which qualitatively follows the theoretical curves obtained by both length-gauge SFA and MO-ADK calculations. However, as compared to HOMO-1 in Fig. 4(a), a more significant difference between the SFA and experimental results can be found for HOMO-2, which may be partially attributed to an intramolecular coupling between the $A^2\Pi_u$ state and excited vibronic levels of the $B^2\Sigma_u$ state [32,33]. In addition, the apparent inconsistency between the experimental measurements and the MO-ADK simulations for the HOMO-1 indicates that the MO-ADK theory, which considers the ionization as a pure tunneling process and has been widely accepted for describing ionization of atoms, may not be able to accurately describe the ionization process of molecules. In contrast, the SFA theory faithfully reproduces the experimental result for HOMO-1, implying that the interference effect, which is inherently accounted for in the SFA theory, plays an essential role in molecular ionization. More detailed analysis is on-going and will be presented elsewhere.

In conclusion, we have shown that the fluorescence emission from molecules provides an efficient way to investigate the alignment-dependent ionization from the lower-lying orbitals. As an all optical means concerning only the wavelengths in the visible and near-ultraviolet regions, the technique is simple. In principle, this technique can be applied to a wide range of molecules (e.g., N_2, O_2, HCl,

H_2O, etc.), as far as their fluorescence emissions are in the suitable spectral ranges and detectable by the available spectrometers. Moreover, it is noteworthy that though the influence of anisotropy on fluorescence radiation itself has been successfully minimized with a back-detection scheme in our experiment for a linear molecule CO_2, it might still add some extra complexities and difficulties for applying this method to more complex molecules, e.g., nonlinear molecules, which remains an interesting topic for further investigation. Because of the exceptionally rich physics in the ionization process of molecules, the unique capability of directly probing the ionization from the lower-lying orbitals in an angular-resolvable manner will provide us not only the potential of retrieval of geometrical information of lower-lying orbitals, but also an ideal test bed for existing theoretical models.

*chen_jing@iapcm.ac.cn
†xjliu@wipm.ac.cn
‡ya.cheng@siom.ac.cn
§zzxu@mail.shcnc.ac.cn

[1] J. Itatani, J. Levesque, D. Zeidler, H. Niikura, H. Pepin, J. C. Kieffer, P. B. Corkum, and D. M. Villeneuve, Nature (London) **432**, 867 (2004).

[2] C. Vozzi, F. Calegari, E. Benedetti, J.-P. Caumes, G. Sansone, S. Stagira, M. Nisoli, R. Torres, E. Heesel, N. Kajumba, J. P. Marangos, C. Altucci, and R. Velotta, Phys. Rev. Lett. **95**, 153902 (2005).

[3] X. M. Tong, Z. X. Zhao, and C. D. Lin, Phys. Rev. A **66**, 033402 (2002).

[4] T. Kanai, S. Minemoto, and H. Sakai, Nature (London) **435**, 470 (2005).

[5] A. Lohr, M. Kleber, R. Kopold, and W. Becker, Phys. Rev. A **55**, R4003 (1997).

[6] F. Krauze and M. Ivanov, Rev. Mod. Phys. **81**, 163 (2009).

[7] I. V. Litvinyuk, K. F. Lee, P. W. Dooley, D. M. Rayner, D. M. Villeneuve, and P. B. Corkum, Phys. Rev. Lett. **90**, 233003 (2003).

[8] S.-F. Zhao, C. Jin, A.-T. Le, T. F. Jiang, and C. D. Lin, Phys. Rev. A **81**, 033423 (2010).

[9] D. Pavičić, K. F. Lee, D. M. Rayner, P. B. Corkum, and D. M. Villeneuve, Phys. Rev. Lett. **98**, 243001 (2007).

[10] S. Petretti, Y. V. Vanne, A. Saenz, A. Castro, and P. Decleva, Phys. Rev. Lett. **104**, 223001 (2010).

[11] C. Vozzi, M. Negro, F. Calegari, G. Sansone, M. Nisoli, S. De Silvestri, and S. Stagira, Nat. Phys. **7**, 822 (2011).

[12] Z. Y. Lin, X. Y. Jia, C. L. Wang, Z. L. Hu, H. P. Kang, W. Quan, X. Y. Lai, X. J. Liu, J. Chen, B. Zeng, W. Chu, J. P. Yao, Y. Cheng, and Z. Z. Xu, Phys. Rev. Lett. **108**, 223001 (2012).

[13] O. Smirnova, Y. Mairesse, S. Patchkovskii, N. Dudovich, D. Villeneuve, P. Corkum, and M. Y. Ivanov, Nature (London) **460**, 972 (2009).

[14] A. E. Boguslavskiy, J. Mikosch, A. Gijsbertsen, M. Spanner, S. Patchkovskii, N. Gador, M. J. J. Vrakking, and A. Stolow, Science **335**, 1336 (2012).

[15] J. Wu, L. Ph. H. Schmidt, M. Kunitski, M. Meckel, S. Voss, H. Sann, H. Kim, T. Jahnke, A. Czasch, and R. Dörner, Phys. Rev. Lett. **108**, 183001 (2012).

[16] H. Akagi, T. Otobe, A. Staudte, A. Shiner, F. Turner, R. Dörner, D. M. Villeneuve, and P. B. Corkum, Science **325**, 1364 (2009).

[17] X. Xie, K. Doblhoff-Dier, S. Roither, M. S. Schöffler, D. Kartashov, H. Xu, T. Rathje, G. G. Paulus, A. Baltuška, S. Gräfe, and M. Kitzler, Phys. Rev. Lett. **109**, 243001 (2012).

[18] J. Yao, B. Zeng, H. Xu, G. Li, W. Chu, J. Ni, H. Zhang, S. L. Chin, Y. Cheng, and Z. Xu, Phys. Rev. A **84**, 051802 (R) (2011).

[19] C. Wu, H. Zhang, H. Yang, Q. Gong, D. Song, and H. Su, Phys. Rev. A **83**, 033410 (2011).

[20] S. Petretti, Y. V. Vanne, A. Saenz, A. Castro, and P. Decleva, Phys. Rev. Lett. **104**, 223001 (2010).

[21] R. A. Bartels, T. C. Weinacht, N. Wagner, M. Baertschy, Chris H. Greene, M. M. Murnane, and H. C. Kapteyn, Phys. Rev. Lett. **88**, 013903 (2001).

[22] F. Calegari, C. Vozzi, S. Gasilov, E. Benedetti, G. Sansone, M. Nisoli, S. De Silvestri, and S. Stagira, Phys. Rev. Lett. **100**, 123006 (2008).

[23] M. W. Schmidt, K. K. Baldridge, J. A. Boatz, S. T. Elbert, M. S. Gordon, J. H. Jensen, S. Koseki, N. Matsunaga, K. A. Nguyen, S. Su, T. L. Windus, M. Dupuis, and J. A. Montgomery, J. Comput. Chem. **14**, 1347 (1993).

[24] T. Seideman, J. Chem. Phys. **103**, 7887 (1995).

[25] J. Ortigoso, M. Rodriguez, M. Gupta, and B. Friedrich, J. Chem. Phys. **110**, 3870 (1999).

[26] B. K. McFarland, J. P. Farrell, P. H. Bucksbaum, and M. Gühr, Science **322**, 1232 (2008).

[27] J. Muth-Böhm, A. Becker, and F. H. M. Faisal, Phys. Rev. Lett. **85**, 2280 (2000).

[28] T. K. Kjeldsen and L. B. Madsen, Phys. Rev. A **71**, 023411 (2005).

[29] W. Becker, J. Chen, S. G. Chen, and D. B. Milošević, Phys. Rev. A **76**, 033403 (2007).

[30] M. Abu-samha and L. B. Madsen, Phys. Rev. A **80**, 023401 (2009).

[31] R. Murray, M. Spanner, S. Patchkovskii, and M. Y. Ivanov, Phys. Rev. Lett. **106**, 173001 (2011).

[32] S. Leach, P. R. Stannard, and W. M. Gelbart, Mol. Phys. **36**, 1119 (1978).

[33] In molecular HHG, dynamical (electronic) effects must be taken into account due to interference between harmonics originated from different orbitals [13]. In contrast, in our technique, the contributions from the different ionization channels are separated because of their characteristic fluorescence wavelengths. Therefore, the dynamical (electronic) effects will not affect our results.